Adsorption of Sarin and Soman on Dickite: An ab Initio ONIOM Study

A. Michalkova,[†,‡] L. Gorb,[‡] M. Ilchenko,[‡] O. A. Zhikol,[§] O. V. Shishkin,[§] and J. Leszczynski*[,‡]

Institute of Inorganic Chemistry, Slovak Academy of Sciences, Dúbravská Cesta 9, 842 36 Bratislava, Slovak Republic, Computational Center for Molecular Structure and Interactions, Department of Chemistry, Jackson State University, 1400 Lynch Street, P.O. Box 17910, Jackson, Mississippi 39217, and Institute for Scintillation Materials, National Academy of Sciences of Ukraine, 60 Lenina Avenue, 61001 Kharkov, Ukraine

Received: March 31, 2003; In Final Form: August 20, 2003

The adsorption of sarin (GB), isopropyl methylphosphonofluoridate ($C_4H_{10}FO_2P$), and soman (GD), 3,3-dimethyl-2-butyl methylphosphonoflouridate ($C_7H_{16}FO_2P$), on the octahedral and tetrahedral surfaces of dickite was investigated using the ONIOM(B3LYP/6-31G(d,p):PM3) and ONIOM(B3LYP/6-31G(d,p):HF/3-21G) methods and the representative cluster models. In the case of adsorption on the octahedral sheet of dickite, the location of six hydrogen atoms of the outer −OH groups and the geometry of the adsorbed molecules were optimized. In the case of adsorption on the tetrahedral side of the dickite layer, the geometry of the mineral fragment was kept frozen. The location and orientation of GB and GD on the tetrahedral and octahedral surfaces of dickite were found. The adsorption on the surface of minerals occurs because of the formation of multiple hydrogen bonds between adsorbed GB and GD and the hydroxyl groups (the octahedral side) and the basal oxygen atoms (the tetrahedral side). This type of adsorption results in the polarization and the electron density redistribution of GB and GD on the surface of the mineral. The interaction energies of sarin and soman with the octahedral and tetrahedral surfaces corrected by the BSSE energy were found. The adsorption energies obtained at the ONIOM(B3LYP/6-31G(d,p):PM3) level of theory and using large models of the mineral for the adsorption systems of GB and GD on the octahedral surface of dickite are about −16 and −15 kcal/mol, respectively. In the case of adsorption on the tetrahedral surface, the interaction energies of adsorption systems with GB and GD are about −7.0 and −9.0 kcal/mol, respectively.

1. Introduction

Clays are layered aluminosilicates showing a large variety of important physicochemical properties: sorption ability, a large specific surface, swelling, the ability to intercalate or to exchange ions and molecules, catalytic properties, and surface acidity.[1,2] Therefore, the clay minerals are used as natural adsorbents and catalysts in industrial applications for the purification and recycling of water systems, disposal of radioactive elements from water, remediation of explosive contaminants, and many other applications.[3,4] The large sorption ability of clay minerals is the reason that these materials can be used to dispose of nerve gases.[5]

The minerals of the kaolinite group can adsorb polar organic molecules relatively easily. Two views of the relaxed structure of the isolated 1:1 layer of the minerals of the kaolinite group, obtained from the total structural relaxation of the isolated layer using ab initio periodic calculations, are displayed in Figure 1, (For more details, see ref 6.) In the ideal case, the layers of these minerals are not charged, and their interlayer space does not contain exchange cations or intercalated molecules. Dickite is a typical representative of minerals of the kaolinite group with a dioctahedral 1:1 layer structure consisting of an octahedral aluminum hydroxide sheet and a tetrahedral silica sheet.[1,2] The tetrahedral side of a layer is characterized by ditrigonal cavities.

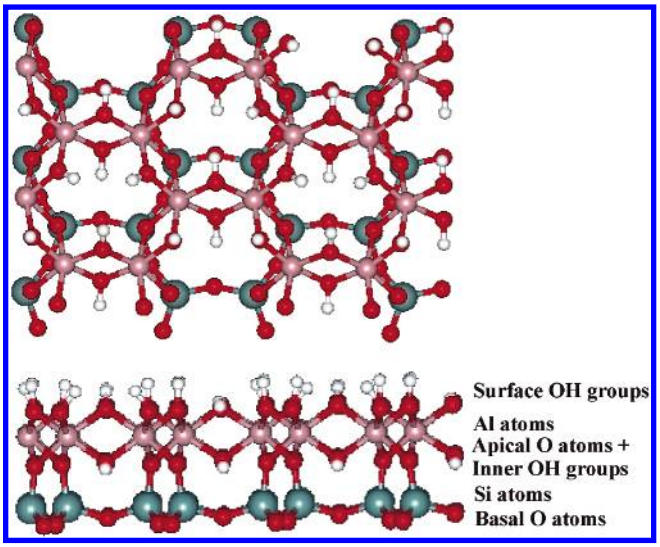

Figure 1. Optimized structure of the isolated 1:1 kaolinite layer: top (upper) and side (lower) views.[6]

The layers are kept together via hydrogen bridges between the surface hydroxyl groups of the octahedral side and the basal oxygen atoms of the tetrahedral side. Therefore, the active sites for adsorption on the clay minerals are hydroxyl groups of the octahedral side and oxygen atoms of the Si−O−Si groups on the tetrahedral side.

Sarin (GB), isopropyl methylphosphonofluoridate ($C_4H_{10}FO_2P$), and soman (GD), 3,3-dimethyl-2-butyl methylphospho-

* To whom correspondence should be addressed. E-mail: jerzy@ccmsi.us. Phone: 001-601-9797824. Fax: 001-601-9797823.
[†] Slovak Academy of Sciences.
[‡] Jackson State University.
[§] National Academy of Science of Ukraine.

10.1021/jp030391e CCC: $27.50
Published on Web 01/15/2004

noflouridate ($C_7H_{16}FO_2P$), are very toxic organophosphorus compounds.[7] These substances are known as nerve agents because of their effects on the disruption of nerve impulses in humans. GB and GD exist in several stereoisomers[8] and conformers.[9] These nerve agents were used in World War I, Laos, Cambodia, Afghanistan, Iran, and Iraq during the Gulf War as lethal chemical warfare weapons. They are intended in military operations to kill, seriously injure, or incapacitate people because of their physiological effects. The major use of chemical weapons at the current time is in the form of terrorist attacks. This was the case in March 1995 in Tokyo, Japan, when a religious cult released a form of sarin nerve gas into Tokyo's subway system.

To the best of our knowledge, there are no investigations of the interaction of sarin or soman with clay minerals. However, several experimental studies of adsorption of phosphate molecules on the surface of clay minerals have been published. We review only a few studies of the interactions of phosphates with montmorillonite because the subject of these studies[10−19] does not directly concern the goal of our study. This clay mineral contains exchangeable cations in the interlayer space that do not occur in the ideal structure of dickite and kaolinite. This could result in different interactions of the organic molecule with the surface of these minerals, which we will discuss elsewhere.[20] Several experiments have been devoted to the study of the interactions of sarin and soman with aqueous soils.[21−24]

Most of the theoretical studies of the interactions between clay minerals and the organic species apply cluster approximations, which prove to be very useful for giving detailed insight concerning the adsorption processes of organic molecules on clay minerals. Despite the utmost importance of nerve agent adsorption on clay mineral surfaces, there are no theoretical studies concerning this phenomenon. Only theoretical studies of the interaction of phosphate with silica and hectorite have been published by Murashov and Leszczynski[25] and by Hartzell and co-workers.[26] The ab initio calculation of hydrogen-bond complexes of dihydrogen and dimethyl phosphate anions with orthosilicic acid have shown that the phosphate groups can form strong hydrogen-bonded complexes with the silanols of the silica surface with stabilization energies of ca. −14 kcal/mol per hydrogen bond.[25] A molecular dynamics study of the large tributyl phosphate complex of europium provides a test of the sensitivity of force field calculations to predict the behavior of molecules within the interlayer of a trioctahedral smectite clay —hectorite.[26] Therefore, this work is intended to attain information concerning the mechanisms of interactions of nerve agents with soils. The first part of such a project is the understanding of the adsorption of sarin and soman on soils, especially on clay minerals, as a consideration for the remediation of contaminants in soils.[5]

2. Computational Details

The geometry optimization was performed using the two-level ONIOM method (*n*-layered integrated molecular orbital and molecular mechanics approach)[27] as implemented in the Gaussian 98 program package.[28] The ONIOM method facilitates calculations of large molecular systems with high accuracy. The ONIOM method is a multilevel extrapolation method in which the studied molecular system is divided into two or more parts or layers. The most important part from a chemical point of view of the system (the inner part, IP) is treated at a "high" level of theory (the HL method, a high level of ab initio molecular orbital method), and the rest of the system is described by a computationally less demanding method (the LL method, the lowest ab initio approximation or semiempirical or molecular mechanics approximations). In the case of the studied systems, the model is divided into the high-level part calculated at the B3LYP level of theory[29,30] with the 6-31G(d,p) basis set and the low-level part calculated using the semiempirical PM3 method[31,32] or the HF/3-21G method. (See Figure 2, which presents the mineral fragment of the adsorption model on the octahedral surface (a) and on the tetrahedral surface (b) of dickite with details concerning the partition of the model into the inner part and boundary part.)

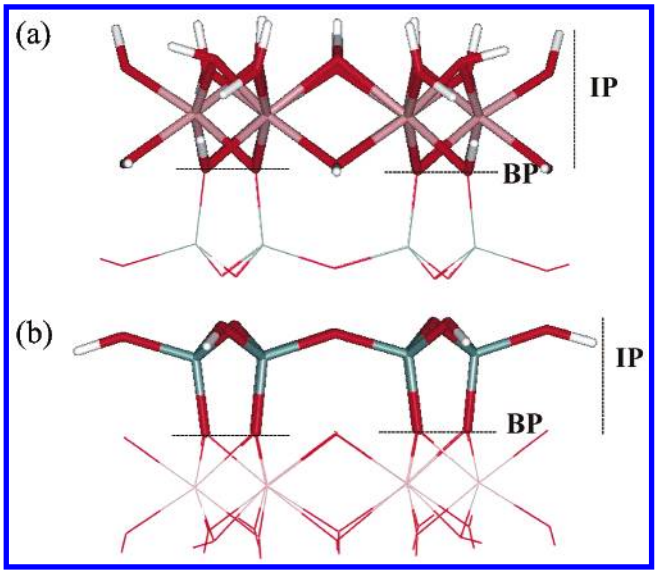

Figure 2. Mineral fragment of the adsorption model on the octahedral surface (a) and on the tetrahedral surface (b) of dickite with details concerning the partition of the model into the inner part (IP) and boundary part (BP).

Two types of cluster models, which we will call large and small, were considered to simulate the surface of dickite. The details of calculated models can be seen in Figures 4−7. The large model (260 atoms) consists of 1 fragment of the 1:1 layer of dickite having 7 silicon−oxygen rings from the tetrahedral sheet and 7 aluminum−oxygen rings from the octahedral sheet. This model was constructed using the structural data of dickite.[33] Dangling bonds of the mineral-layer fragments were saturated with hydrogen atoms. The chemical formula of the mineral fragment of this model is $Si_{24}Al_{24}O_{126}H_{84}$. The small model of the mineral (78 atoms) consists of 1 middle silicon−oxygen ring of the tetrahedral sheet and 1 middle aluminum−oxygen ring of the octahedral sheet of the large model. The chemical formula of this model is $Si_6Al_6O_{36}H_{30}$. Abbreviations for calculated adsorbed systems and chemical formulas of the inner mineral fragment of the model are presented in Table 1. For practical reasons, we will use the notation R for the $-CH(CH_3)_2$ fragment of GB and for the $-CH(CH_3)-C(CH_3)_3$ fragment of GD.

GB and GD were allowed to relax fully. In addition, the positions of the hydrogen atoms of the six surface −OH groups of dickite were optimized in the case of the adsorption on the octahedral surface. In the case of adsorption on the tetrahedral side of the dickite layer, the geometry of the clay-layer cluster was kept frozen. The interaction energy was corrected to the basis set superposition error (BSSE) using the counterpoise method.[34] The nature of the interactions was studied using the decomposition scheme proposed by Sokalski et al.[35] and the inner part of optimized models at the B3LYP/6-31G(d,p) level. In this approach, the self-consistent field (SCF) interaction energy is partitioned into the first-order electrostatic $\epsilon_{el}^{(10)}$, the

TABLE 1: Abbreviations of Calculated Adsorption Systems Used in the Text and Chemical Formulas of the Inner Mineral Fragment of the Model

investigated system	abbreviation	composition of the inner mineral part[a]
dickite(octahedral side)−large model with seven tetrahedral and octahedral rings−sarin	D7(o)-GB	$Al_6(OH)_{14}O_{10}H_{16}$
dickite(octahedral side)−large model with seven tetrahedral and octahedral rings−soman	D7(o)-GD	$Al_6(OH)_{14}O_{10}H_{16}$
dickite(tetrahedral side)−large model with seven tetrahedral and octahedral rings−sarin	D7(t)-GB	$Si_6O_{12}H_{12}$
dickite(tetrahedral side)−large model with seven tetrahedral and octahedral rings−soman	D7(t)-GD	$Si_6O_{12}H_{12}$
dickite(octahedral side)−small model with one tetrahedral and octahedral ring−sarin	D(o)-GB	$Al_6(OH)_{14}O_{10}H_{16}$
dickite(octahedral side)−small model with one tetrahedral and octahedral ring−soman	D(o)-GD	$Al_6(OH)_{14}O_{10}H_{16}$
dickite(tetrahedral side)−small model with one tetrahedral and octahedral ring−sarin	D(t)-GB	$Si_6O_{12}H_{12}$
dickite(tetrahedral side)−small model with one tetrahedral and octahedral ring−soman	D(t)-GD	$Si_6O_{12}H_{12}$
dickite(octahedral side)−small model with one tetrahedral and octahedral ring with different initial position of adsorbed molecule−sarin	D′(o)-GB D″(o)-GB D‴(o)-GB	$Al_6(OH)_{14}O_{10}H_{16}$
dickite(tetrahedral side) small model with one tetrahedral and octahedral ring with different initial position of adsorbed molecule−sarin	D′(t)-GB	$Si_6O_{12}H_{12}$

[a] With the inclusion of terminal hydrogen atoms and with the exclusion of the organic molecule.

Heitler−London exchange ϵ_{ex}^{HL}, and the higher-order delocalization ΔE_{del}^{HF} energy terms defined for the whole system basis set. The ΔE_{del}^{HF} delocalization term accounts for the exchange transfer and the induction interaction associated with the relaxation of the electronic densities of the subsystem upon interaction and other higher-order Hartree−Fock terms.[36] To take into account the correlation energy, the former scheme was augmented by the second-order intermolecular dispersion[36] ($\epsilon_{disp}^{(20)}$) and the correlation correction on the SCF interaction energy calculated on the basis of the MP2 method ($\epsilon_{MP}^{(2)}$). The $\epsilon_{MP}^{(2)}$ energy term includes the dispersion contribution and the higher-order correlation energy components, and it is calculated as a difference between the MP2 and SCF interaction energies calculated consistently for the basis set of the whole system.[37]

We also have analyzed atomic charges of the inner parts of adsorption systems D-GB and D-GD using the Mulliken population analysis as implemented in the Gaussian 98 program package[28] at the B3LYP/6-31G(d,p) level. The topological characteristics of the electron density distribution were obtained following Bader's atoms in molecules approach (AIM)[38] at the same level of theory.

3. Results and Discussion

To estimate the accuracy of the results obtained at the B3LYP level for weakly interacting models (the adsorption on the tetrahedral surface) relative to the results obtained at the MP2/6-31G(d,p) level, we have performed additional calculations of the interaction of sarin with one SiO_4 tetrahedra of the tetrahedral ring. The dangling bonds of this model were saturated by hydrogen atoms. At both levels, similar optimized structures, positions, and interactions of sarin with tetrahedra have been found. The optimized structure is presented in Figure 3. The difference in the geometrical parameters of sarin is about 1%. The MP2 and DFT results differ in values of the interaction energy (−8 kcal/mol (B3LYP) and −4.1 kcal/mol (MP2)) and in hydrogen bond distances (1.778 Å (B3LYP) and 1.804 Å (MP2)). One can see that the calculation at the B3LYP level largely overestimates the value of the interaction energy of the weakly interacting adsorption systems with the large organic molecule. The overestimation of the strength of the hydrogen bonds is about 10% compared to the results obtained at MP2 level. The statement concerning the overestimation of the interaction energy is in agreement with a finding of the study of the formamide dimer by Michalkova et al.[39]

Recently, the population of the conformational space of isolated sarin and soman was determined in high-level-correlated ab initio calculations.[9] Three low-energy conformers, which differ in the orientation of the R group, have been found for both molecules. However, our calculations reveal that the orientation of the R group does not change our results concerning interactions of GB and GD with the dickite surface at all because the most important contribution to the interaction energy comes from the interaction between the P═O group and OH groups of the octahedral surface. Therefore, in our investigations we used the most stable conformers of GB and GD.

3.1. Geometrical Parameters (General Consideration). Figures 4−7 show two views of the optimized structures of adsorbed GB and GD on the octahedral and tetrahedral surfaces of dickite, calculated using the ONIOM(B3LYP/6-31G(d,p): PM3) method (the D7(o)-GB, D7(o)-GD, D7(t)-GB, and D7-(t)-GD models).

An analysis of the data presented in Tables 2 and 3, which contain geometrical parameters of adsorbed and isolated sarin and soman, and in Figures 4−7 enables us to make the following statement. The interactions of GB and GD with a large cluster model, mimicking the octahedral and tetrahedral surfaces of dickite, result in the same geometry characteristics of the adsorbed molecule as those that were obtained using the small ones. Only insignificant differences in the geometric parameters of GB and GD were observed. For example, the maximum difference between the bond lengths of adsorbed GB and GD obtained using large models and small models is about 0.01 Å (about 5° for the angles). This indicates that the surrounding octahedral and tetrahedral rings have virtually no influence on the structure of adsorbed GB and GD. According to this result, one can conclude that such cluster models (D(o)-GB, D(o)-GD, D(t)-GB, and D(t)-GD) are sufficient for a description of the

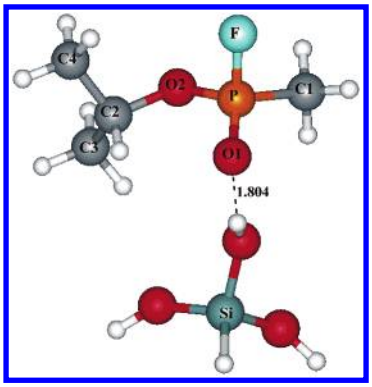

Figure 3. Optimized structure of the sarin−tetrahedra system obtained at the MP2/6-31G(d,p) level.

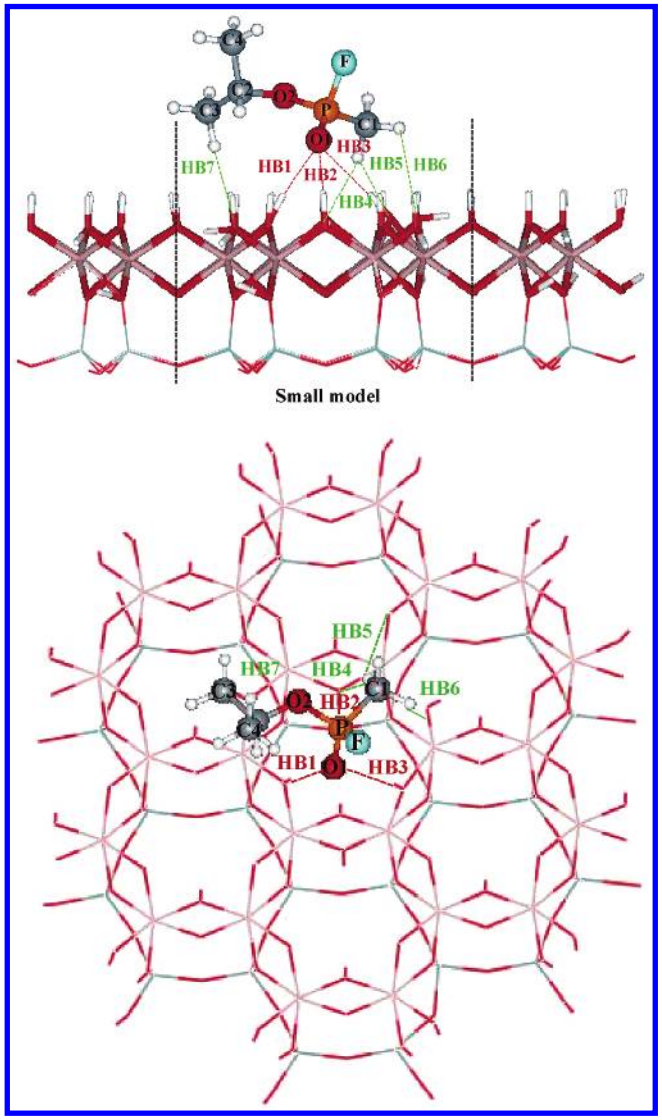

Figure 4. Dickite−sarin adsorbed system on the octahedral surface—D7(o)-GB. Two views of the cluster model in optimized geometry obtained using the ONIOM(B3LYP/6-31G(d,p):PM3) method.

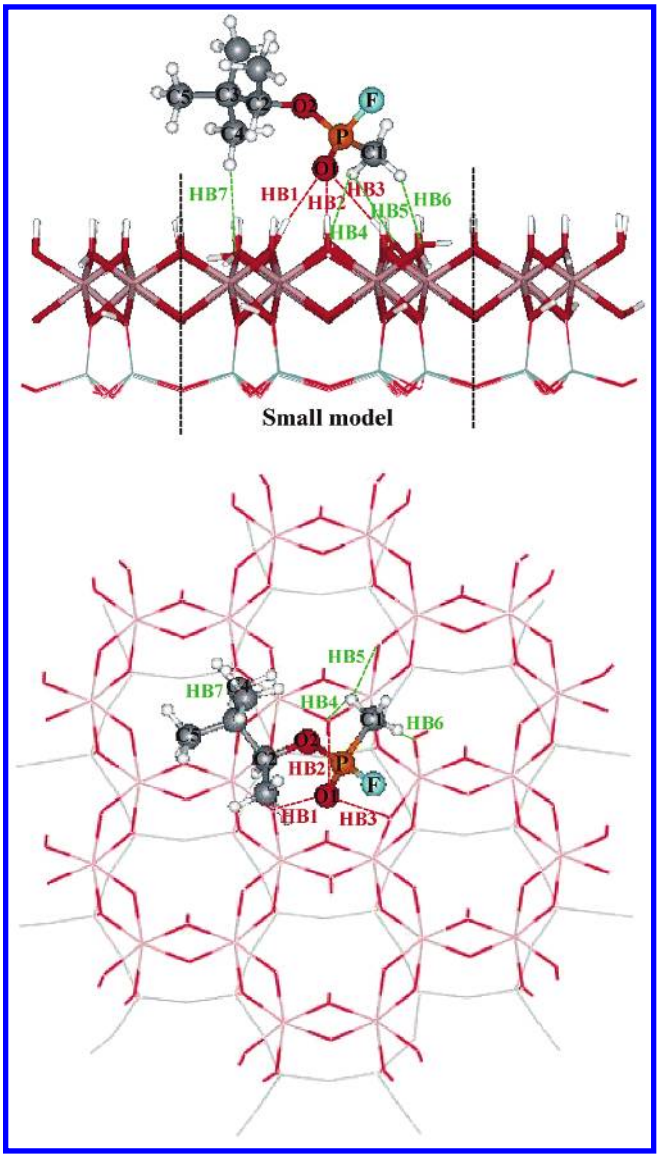

Figure 5. Dickite−soman adsorbed system on the octahedral surface—D7(o)-GD. Two views of the cluster model in optimized geometry obtained using the ONIOM(B3LYP/6-31G(d,p):PM3) method.

geometrical parameters of the adsorption of GB and GD on clay minerals. A similar conclusion was obtained in the theoretical studies of dickite and kaolinite with several organic species and water.[39−41] In addition, it was found that an investigation of the considered models using two ONIOM approximations, B3LYP/6-31G(d,p):PM3 and B3LYP/6-31G(d,p):HF/3-21G, which differ only in the low ONIOM level, provides virtually the same results concerning the location, orientation, and structure of adsorbed molecules on the surface of dickite with insignificant differences in its composition geometry parameters (Tables 2 and 3).

Let us now describe the location of adsorbed sarin and soman on the surface of dickite. The structure and orientation of these adsorbed molecules correspond to their ability to form attractive contacts with the surface of dickite. One can see that these molecules are placed above the octahedral hole of dickite in such a way that the O1 atom of the organic molecule is directed into the center of the octahedral cavity (Figures 4 and 5). The P−C bonds of GB and GD are almost parallel to the surface of dickite.

The locations of GB and GD on the tetrahedral surface of dickite are different than the adsorption of GB and GD on the octahedral surface (Figures 6 and 7). The $-CH_3$ group of GB in the D7(t)-GB complex is located above the center of the ditrigonal cavity so that the (PO2C2) plane is almost parallel to the plane of the basal oxygen atoms of dickite. In the case of the D7(t)-GD system, the R group is extended to cover the whole ditrigonal cavity so that one CH_3 group (the C5 carbon atom) of this R group is oriented with respect to the center of this

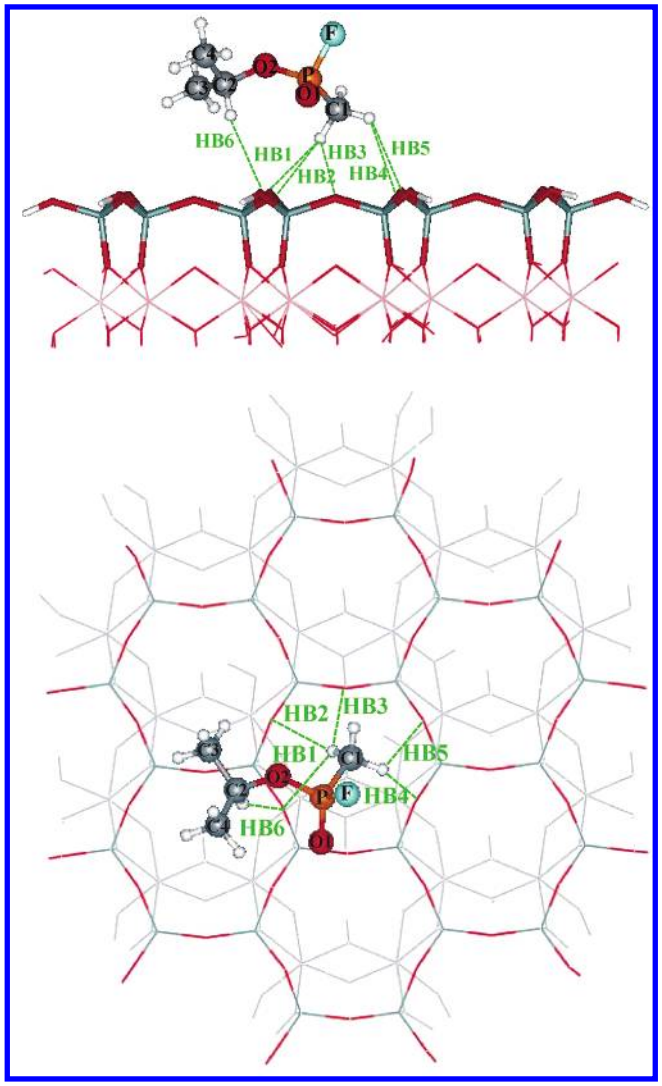

Figure 6. Dickite−sarin adsorbed system on the tetrahedral surface−D7(t)-GB. Two views of the cluster model in optimized geometry obtained using the ONIOM(B3LYP/6-31G(d,p):PM3) method.

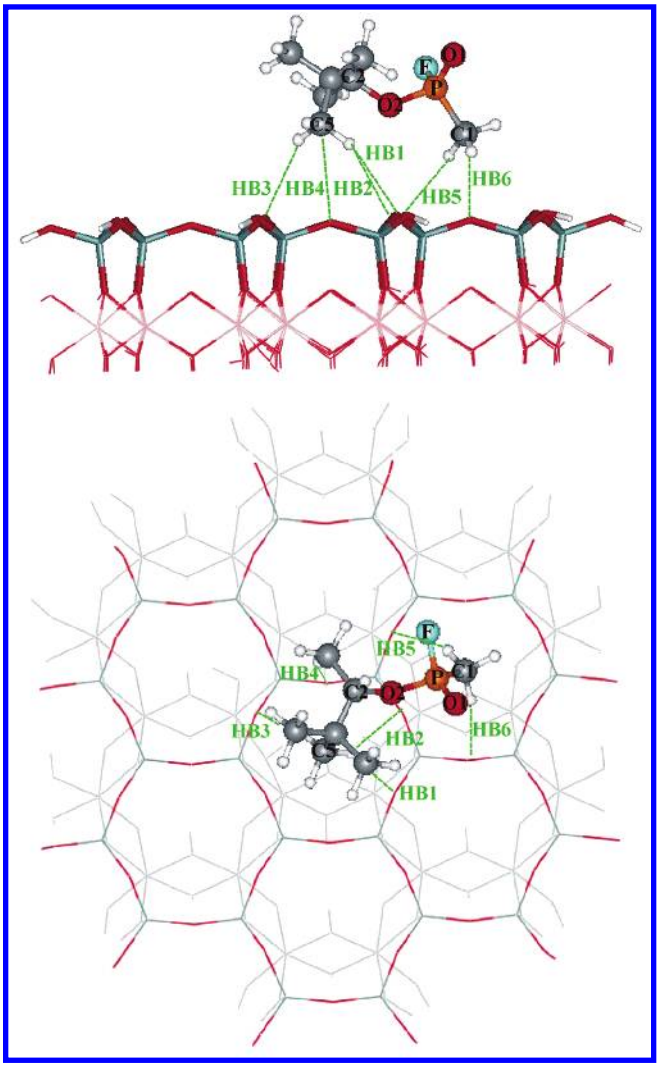

Figure 7. Dickite−soman adsorbed system on the tetrahedral surface−D7(t)-GD. Two views of the cluster model in optimized geometry obtained using the ONIOM(B3LYP/6-31G(d,p):PM3) method.

cavity. Because of steric reasons, the rest of the adsorbed GD is located on the outside area of the tetrahedral ring.

3.2. Hydrogen Bonds between Sarin, Soman, and Dickite. *3.2.1. AIM Analysis of Multiple Hydrogen Bonds*. As follows from the data presented in Figures 4−7, the adsorption on both the octahedral and tetrahedral sites of dickite occurs through the formation of multiple hydrogen bonds.

Unfortunately, the complex character of the interactions of GB and GD molecules with the clay surfaces does not allow the exact number of hydrogen bonds that will be formed between adsorbed molecules and the surface of clay minerals to be determined. However, such an analysis is possible on the basis of the atoms in molecules theory.[38] The AIM analysis includes the location of the so-called (3, −1) bond critical points (BCPs) on the surface of the total charge density, the analysis of the electron density (ρ), the analysis of the Laplacian of electron density ($\nabla^2\rho$) at BCPs, distances of H bonds, and changes in electron density on hydrogen atoms involved in the formation of hydrogen bonds. (For several more criteria of hydrogen bonding, see refs 42 and 43.) The existence of the (3, −1) BCP indicates the formation of chemical bonds independently of its nature.[38]

The application of the AIM analysis reveals the appearance of several (3,−1) BCPs that could be related to hydrogen bonds of different types between sarin and soman and the surface of dickite. All of them are presented in Table 4, denoted as HB1−HB7.They are characterized by their values of ρ and $\nabla^2\rho$, which are crucial to the formation of hydrogen bonds of any type.[42] In addition, the positive value of $\nabla^2\rho$ should also be in the range that is typical for the formation of hydrogen bonds. As follows from the AIM analysis presented in refs 42 and 43 in the case of the formation of O−H···O hydrogen bonds, the values of charge density at BCP should be about an order of magnitude smaller than those found for covalent bonds. Therefore, during the adsorption of GB and GD on the octahedral surface of dickite, there are three hydrogen bonds of this type, denoted as HB1−HB3. They are formed between the O1 atoms of sarin and soman and hydroxyl groups on the surface of dickite. We expect that these H bonds contribute mostly to the stabilization energy of the GB and GD molecules on the surface of dickite. In this case, the O1 atoms of GB and GD act as proton acceptors, and the hydroxyl groups on the surface act as proton donors.

In the case of the formation of the C−H...O type of hydrogen bond, the ρ value should be approximately 5 times smaller than the one corresponding to the O−H···O type of hydrogen bond. Therefore, the hydrogen bonds, denoted as HB4−HB7, should be classified as this particular kind. These interactions provide an additional contribution to the interaction energy of the studied systems. In the case of both the D-GB and D-GD systems, three

TABLE 2: Geometric Parameters of Adsorbed GB Obtained Using the ONIOM(B3LYP/6-31G(d,p):PM3) and ONIOM(B3LYP/6-31G(d,p):HF/3-21G) Methods and Isolated GB Calculated at the B3LYP/6-31G(d,p) Level of Theory

system	D(o)-GB		D7(o)-GB	D(t)-GB		D7(t)-GBGB	
parameters[a]/ LL method	PM3	HF	PM3	PM3	HF	PM3	GB
D(P═O1)	1.492	1.498	1.486	1.482	1.483	1.481	1.478
D(P−F)	1.603	1.594	1.610	1.604	1.606	1.602	1.600
D(P−O2)	1.612	1.600	1.596	1.606	1.608	1.599	1.604
D(P−C1)	1.785	1.788	1.777	1.792	1.794	1.789	1.802
D(C2−O2)	1.469	1.474	1.470	1.463	1.461	1.472	1.469
D(C2−C3)	1.523	1.521	1.519	1.524	1.525	1.524	1.524
D(C1−H)[b]	1.094	1.093	1.093	1.092	1.091	1.094	1.092
D(C3−H)[b]	1.094	1.094	1.095	1.094	1.095	1.095	1.094
α(O1−P−C1)	121.6	119.5	120.5	119.2	119.4	118.7	118.3
α(O1−P−O2)	115.4	114.5	116.9	115.9	116.0	116.8	116.9
α(O1−P−F)	108.7	109.3	108.6	111.4	110.8	111.3	112.4
α(P−O2−C2)	121.6	121.6	122.3	120.7	121.1	122.6	120.6
γ(O1−P−C1−O2)	132.2	129.4	133.3	130.8	130.8	134.6	130.2
γ(O1−P−F−O2)	−122.5	−122.7	−124.0	−124.2	−124.2	−123.2	−126.6
γ(F−P−C1−O2)	−106.3	−108.6	−106.0	−105.9	−106.1	−102.8	−106.1

[a] Bond lengths (*D*) are in angstroms, and angles (α) and dihedral angles (γ) are in degrees. [b] Average value.

TABLE 3: Geometric Parameters of Adsorbed GD Obtained Using the ONIOM(B3LYP/6-31G(d,p):PM3) and ONIOM(B3LYP/6-31G(d,p):HF/3-21G) Methods and Isolated GD Calculated at the B3LYP/6-31G(d,p) Level of Theory

system	D(o)-GD		D7(o)-GD	D(t)-GD		D7(t)-GD	
parameters[a]/ LL method	PM3	HF	PM3	PM3	HF	PM3	GD
D(P−O1)	1.493	1.498	1.484	1.486	1.482	1.484	1.478
D(P−F)	1.599	1.593	1.605	1.612	1.609	1.606	1.600
D(P−O2)	1.606	1.597	1.601	1.608	1.605	1.603	1.604
D(P−C1)	1.788	1.789	1.778	1.791	1.792	1.779	1.802
D(C3−C4)	1.543	1.543	1.544	1.540	1.540	1.543	1.543
D(C3−C5)	1.542	1.542	1.542	1.542	1.542	1.540	1.542
D(C1−H)[b]	1.094	1.092	1.094	1.094	1.094	1.096	1.092
D(C4−H)[b]	1.096	1.093	1.096	1.095	1.094	1.096	1.095
D(C5−H)[b]	1.095	1.095	1.095	1.095	1.094	1.095	1.095
α(O1−P−C1)	122.2	119.6	121.4	119.4	119.5	118.7	118.3
α(O1−P−O2)	114.8	114.7	115.3	121.2	116.5	115.6	117.0
α(P−O2−C2)	123.4	123.3	122.9	116.5	121.5	122.9	120.8
γ(O1−P−C1−O2)	131.1	129.3	132.1	131.2	131.2	130.6	130.4
γ(O1−P−F−O2)	−122.2	−123.2	−122.3	−124.9	−124.7	−123.0	−126.6
γ(F−P−C1−O2)	−106.5	−108.6	−105.4	−106.2	−106.2	−106.6	−106.0

[a] Bond lengths (*D*) are in angstroms, and angles (α) and dihedral angles (γ) are in degrees. [b] Average value.

prospective C−H···O bonds (HB4, HB5, and HB6) include the interactions of hydrogen atoms belonging to the CH_3 group (the $-C_1$ carbon atom) as proton donors with the oxygen atoms of the hydroxyls (proton acceptors). The remaining HB7 bond is different for the D7(o)-GB and D7(o)-GD adsorption systems. In the case of the D-GB system, this is the interaction between the C3−H fragment of sarin and the oxygen atom of the surface hydroxyl. In the case of the D-GD system, this is the H bond between the oxygen atom of the surface hydroxyl and the C4−H group of soman. Both C−H···O and O−H···O are disposed toward a linear arrangement of these three atoms, although the former can be more easily bent (Figures 4 and 5). Similar details of the formation of hydrogen bonds were found using the small and large cluster models of the octahedral side of dickite. However, one can expect that because of the large size of the molecule there are some additional interactions with the surrounding tetrahedral and octahedral rings of dickite.

An analysis of the nature of (3, −1) BCPs that characterize the adsorption of GB and GD on the tetrahedral surface of dickite suggests that the molecule forms only the C−H...O type of hydrogen bonds with the surface. (See notations HB1−HB6 in Table 4 for the D7(t)-GB and D7(t)-GD models.) In this case, the AIM analysis reveals that the CH_3 groups of GB and GD play the main role in the formation of H bonds with the surface. The tetrahedral surface does not contain hydroxyl groups that are responsible for the formation of hydrogen bonds with GB and GD in the case of the adsorption on the octahedral surface. The active sites on the tetrahedral surface of dickite are basal oxygen atoms. The C1−H fragment of GB and GD acts as a proton donor in D7(t)-GB and D7(t)-GD models, forming multiple weak H-bonds with basal oxygen atoms of the dickite surface (HB1−HB5 bonds in the D7(t)-GB model and HB5 and HB6 bonds in the D7(t)-GD model in Table 4). In addition, the HB6 bond (the D-GB system) and HB1−HB3 bonds (the D-GD system), formed between the C2−H fragment of GB or the C5−H fragments of GD and the tetrahedral side, also contribute to the stabilization of these molecules on the surface of dickite. In both cases of the adsorption systems, different orientations of the molecules were found in comparison with the results obtained using the small and large models. (A more significant difference was found for the D-GD system.) This indicates that the surrounding rings significantly affect the large molecule on the tetrahedral surface (weakly interacting models). The application of a large cluster (relative to the size of the target molecule) causes the involvement of different groups in the intermolecular interactions.

TABLE 4: Calculated ONIOM(B3LYP/6-31G(d,p):PM3) H···Y and X···Y[a] Distances (Å), X−H···Y Angles (deg), and Electron Density Characteristics[b] ρ (au) and $\nabla^2\rho$ (au) of Hydrogen Bonds in D-GB and D-GD Systems

	D7(o)-GB				D7(t)-GB			
	H···Y (X···Y)	X−H···Y	ρ	$\nabla^2\rho$	H···Y (X···Y)	X−H···Y	ρ	$\nabla^2\rho$
HB1	2.003 (2.964)	171.9	0.0207	0.0659	2.85 (3.68)	132.6	0.0035	0.0154
HB2	3.124 (3.591)	111.4	0.0283	0.0857	2.732 (3.785)	161.3	0.0078	0.0266
HB3	2.311 (3.268)	170.3	0.0208	0.0600	2.759 (3.551)	129.0	0.0066	0.0249
HB4	2.207 (3.218)	152.2	0.0060	0.0219	2.726 (3.561)	133.0	0.0041	0.0153
HB5	3.039 (3.966)	142.5	0.0089	0.0247	3.068 (3.65)	113.9	0.0038	0.0149
HB6	2.787 (3.259)	105.9	0.0081	0.0303	2.738 (3.746)	153.0	0.0061	0.0236
HB7	2.578 (3.648)	165.1	0.0054	0.0211				
	D7(o)-GD				D7(t)-GD			
	H···Y (X···Y)	X−H···Y	ρ	$\nabla^2\rho$	H···Y (X···Y)	X−H···Y	ρ	$\nabla^2\rho$
HB1	1.990 (2.947)	170.1	0.0201	0.0667	2.928 (3.915)	150.2	0.0047	0.0166
HB2	3.001 (3.478)	111.8	0.0287	0.0889	3.195 (4.149)	146.1	0.0042	0.0158
HB3	2.175 (3.137)	172.4	0.0193	0.0548	2.907 (3.878)	147.8	0.0033	0.0127
HB4	2.478 (3.205)	122.8	0.0047	0.0185	3.018 (4.055)	158.3	0.0047	0.0186
HB5	3.130 (3.87)	125.5	0.0067	0.0199	2.833 (3.871)	158.1	0.0131	0.0385
HB6	2.188 (3.150)	144.9	0.0088	0.0326	2.656 (3.683)	155.5	0.0139	0.0401
HB7	2.837 (3.905)	164.0	0.0069	0.0254				

[a] In parentheses. [b] Inner part, B3LYP/6-31G(d,p).

In addition, as should be obvious, the low ρ and $\nabla^2\rho$ values characterizing the C−H···O hydrogen bonds compared to values of electron density and the Laplacian of electron density characterizing the O−H···O hydrogen bonds demonstrate that the C−H···O bonds are much weaker.

Table 4 contains calculated H···Y distances, X···Y distances in parentheses, and X−H···Y hydrogen bond angles between GB and GD and the surface of dickite. One can see that the H bonds formed between the O1 atoms of GB and GD and the OH groups of dickite, denoted HB1−HB3 in the case of adsorption on the octahedral side, are the strongest. (The H···O distance is about 2 Å.) The C−H···O hydrogen bonds (the HB4−HB7 bonds in the D7(o)-GB and D7(o)-GD systems and the HB1−HB6 bonds in the D7(t)-GB and D7(t)-GD systems) appear to be weaker than conventional hydrogen bonds. The calculated C−H···O hydrogen bonds between the C−H groups of sarin and soman and the oxygen atoms of the surface of dickite are characterized by longer O···H distances (2.2−3.1 Å). The weaker hydrogen bonds with longer distances correspond to the lower values of ρ and $\nabla^2\rho$ with some discrepancies (for example, the case of the HB2 bond in the D7(o)-GD system), as one can see from Table 4. However, the values of the topological characteristics are influenced by the position of the atoms forming H bonds in the cluster because the border conditions affect the density and Laplacian of electron density around these atoms. HB5 (in the D7(o)-GB and D7(o)-GD models) and HB6 bonds (in the D7(t)-GD model) are formed by the basal oxygen atoms that are on the border between the inner and outer parts of the cluster. In the case of these H bonds, the values of ρ and $\nabla^2\rho$ are higher in comparison with the values predicted for the other H bonds formed by the basal oxygen atom inside the ring, despite similar H···Y distances (for example, HB5 in the D7(o)-GB and D7(t)-GB models). The calculated C···O distances in both the D-GB and D-GD systems range from 3.0 to 4.1 Å. This corresponds well with the interval quoted by Desiraju of 3.0−4.0 Å, which is based on a survey of over 100 structures.[44] Therefore, in the case of adsorption on the tetrahedral surface of dickite, the sarin and soman subsystems and the mineral subsystem are far apart. For example, the shortest H···O distance between the hydrogen atom of the C1−H group and the basal oxygen atom from the surface is about 2.7 Å for the D7(t)-GB and D7(t)-GD systems. The reason for the formation of such weak H bonds is the relatively large molecular volume of sarin and soman, which prevents these species from forming stronger contacts with the surface of dickite. The use of the PM3 approximation as the LL method in the ONIOM calculation yields bond lengths of H bonds between C−H groups of sarin and soman and basal oxygen atoms of the tetrahedral side in the D(t)-GB and D(t)-GD models that are larger by about 5% in comparison with the results obtained using the HF/3-21G method.

Let us estimate the internal fraction of electron density transfer as compared to the amount of density that transfers from one subsystem to another. The sum of atomic charges is zero in the isolated subsystem; its magnitude in the system is an estimate of the amount of density that transfers from one subsystem to the other. Therefore, the latter transfer is calculated as the sum of Mulliken atomic charges on adsorbed sarin and soman. Table 5 reports the values of electron-density transfer from the mineral subsystem to sarin and soman as a consequence of the adsorption of these molecules on the surface of dickite. In the case of D7(o)-GB and D7(o)-GD systems, the O1···H−O hydrogen bonds

TABLE 5: Electron Density Transfer (*me*) from the Mineral Subsystem to Sarin and Soman Obtained Using Mulliken Population Analysis

system	D(o)-GB	D7(o)-GB	D(t)-GB	D7(t)-GB	D(o)-GD	D7(o)-GD	D(t)-GD	D7(t)-GD
transfer	33	23	−10	−13	44	28	−47	−24

TABLE 6: Changes in Mulliken Atomic Charges (*me*) of X, H, and Y Atoms of X−H···Y Hydrogen Bonds in the D-GB and D-GD Systems Relative to Those in Subsystems

system	D7(o)-GB			D7(t)-GB		
bond/transfer	Δq_X	Δq_H	Δq_Y	Δq_X	Δq_H	Δq_Y
HB1	−58	57	−29	−16	13	−32
HB2	−59	48	−29	−16	13	−27
HB3	−63	36	−29	−16	13	−14
HB4	−28	41	−59	−16	15	−15
HB5	−28	41	−29	−16	15	−11
HB6	−28	11	−14	4	9	−32
HB7	−20	24	−32			

system	D7(o)-GD			D7(t)-GD		
bond/transfer	Δq_X	Δq_H	Δq_Y	Δq_X	Δq_H	Δq_Y
HB1	−57	58	−38	−24	27	−6
HB2	−53	46	−38	−24	27	−20
HB3	−70	41	−38	−24	15	−11
HB4	−31	10	−56	−5	29	−15
HB5	−31	10	−24	−21	14	−8
HB6	−31	38	−21	−21	22	−9
HB7	−26	24	−29			

play the main role in the stabilization of sarin and soman on the surface of dickite in comparison with weak C−H···O hydrogen bonds. Therefore, stronger interactions lead to progressively larger density transfers. Such adsorption results in the positive charge of sarin and soman. However, both sarin and soman adsorbed on the tetrahedral surface become negative because of the formation of only C−H···O hydrogen bonds between the C−H groups (proton donors) of GB and GD and the basal oxygen atoms (proton acceptors) of the tetrahedral side. Upon the formation of the adsorption complex, one can see that there are electron density transfers from the proton acceptor to the donor part in formed H bonds. Sarin and soman show few distinguishing proton-acceptor and proton-donor properties. One can see that the electron-density transfer is more significant in the case of the adsorption of soman on the surface of dickite in comparison with that of the sarin adsorption complexes. The greater atomic charge changes of soman can be attributed to the polarization of next three methyl groups.

The transfer of electron density may also be quantified by considering the charges on the individual atoms. The changes in Mulliken atomic charges of X, H, and Y atoms of the X−H···Y hydrogen bonds in the D-GB and D-GD systems relative to those of the isolated organic molecular subsystem and the mineral subsystem are presented in Table 6. One can see that the bridging H atom becomes more positive and that the X and Y atoms become more negative (except for the X atom involved in HB6 of the D7(t)-GB model). This trend is similar in both the D-GB and D-GD systems. The charge changes of the proton donor and acceptor are larger for the O1···H−O hydrogen bonds of the adsorption complexes on the octahedral surface than for the weaker C−H···O interactions. The charge increase on the H atoms results in a hydrogen that is more strongly attracted to the negatively charged O atom.

The formation of hydrogen bonds with the oxygen atom on the border between the inner and outer parts of the cluster (the HB5 in the D7(o)-GB and D7(o)-GD models and HB6 in the D7(t)-GD model) results in an increase in atomic charges on X, H, and Y atoms in comparison with that of the other H bonds characterized by similar H···Y distances (for example, HB5 in the D7(o)-GD model and HB2 in the D7(t)-GD model) because in this case the electron density is influenced by atoms of the inner part and the outer part.

3.2.2. Changes in the Geometry of Sarin and Soman. The formation of hydrogen bonds between GB and GD and the surface of dickite results in changes in the conformation and geometry parameters of the studied molecules in comparison with the gas phase parameters (Tables 2 and 3). This effect is more significant in the case of adsorption on the octahedral surface. The C−H and P═O bonds of adsorbed GB and GD in the case of adsorption on the octahedral surface directly involved in the formation of the hydrogen bonds are lengthened in comparison with the bond lengths of the isolated molecule (Tables 2 and 3). For example, the P═O bond is lengthened by approximately 0.01 Å in the D7(o)-GB and D7(o)-GD systems. The changes, caused by the formation of C−H···O bonds, are less significant than those caused by the O−H···O bonds in the case of adsorption on the octahedral surface. In the case of adsorption on the tetrahedral surface, the P−C1 bond is shortened, and the P═O1 and P−F bonds of the adsorbed molecule are lengthened in comparison with those of isolated GB and GD. The surface of dickite has the same significant influence on the changes in the geometry of GB and GD.

3.2.3. Energetics. The calculation of the interaction energies of the D-GB and D-GD systems reveals that GB and GD interact relatively strongly with the octahedral surface of dickite. (See Table 7, which contains BSSE-corrected interaction energies of the D-GB and D-GD systems calculated using the ONIOM-(B3LYP/6-31G(d,p):PM3) and ONIOM(B3LYP/6-31G(d,p):HF/3-21G) methods.) One can see that for steric reasons GB is better located on the octahedral surface than GD. Interaction energies obtained for the D7(t)-GB and D7(t)-GD models (−7.4 and −9.1 kcal/mol, respectively, using the ONIOM(B3LYP/6-31G(d,p):PM3) method) reveal that soman is better stabilized on the tetrahedral surface of dickite than sarin because of the formation of stronger H bonds with the basal oxygen atoms of the surface. The interaction energies in the case of adsorption on the octahedral surface are twice as large as in the case of the adsorption on the tetrahedral surface as a consequence of the formation of only very weak (a fraction of a kcal/mol) C−H···O hydrogen bonds. This result agrees with the finding of theoretical studies of the adsorption sites on the surface of 1:1 clay minerals[40,41] where the interaction energy of the adsorption system of the water molecule on the octahedral side of the kaolinite layer is stronger by a factor of 2 than on the tetrahedral side. Therefore, we can conclude that GB and GD will preferably be adsorbed on the octahedral side of the clay mineral.

The values of the interaction energy obtained using the large models are larger (in absolute value) than those obtained using the small ones. BSSE-corrected adsorption energies of small models are twice as large as in the case of large models in both cases. The difference is more significant for the D-GD complex. This large difference in adsorption energies is caused by the limitation of the cluster approximation. Because of the large size of sarin and soman, in addition to interactions with the surface of dickite, there are also non-negligible interactions with the border atoms of the small model. Therefore, some important contributions can arise from the interactions of the target

TABLE 7: BSSE-Corrected Interaction Energies (kcal/mol) of the D-GB and D-GD Systems Calculated Using the ONIOM(B3LYP/6-31G(d,p):PM3) and ONIOM(B3LYP/6-31G(d,p):HF/3-21G) Methods

system	D(o)-GB		D7(o)-GB	D(t)-GB		D7(t)-GB	D(o)-GD		D7(o)-GD	D(t)-GD		D7(t)-GD
LL method	PM3	HF	PM3	PM3	HF	PM3	PM3	HF	PM3	PM3	HF	PM3
int. energy	−12.8	−13.0	−16.5	−3.9	−4.9	−7.4	−7.4	−9.9	−15.2	−4.0	−5.7	−9.1

TABLE 8: Decomposition of the Interaction Energy Obtained Using the Optimized (B3LYP/6-31G(d,p)) Inner Part of Models of the D-GB System[a]

system/energy	$\epsilon_{el}^{(10)}$	ϵ_{ex}^{HL}	ΔE_{del}^{HF}	ΔE_{SCF}	$\epsilon_{MP}^{(2)}$	ΔE_{MP2}
D(o)-GB	−29.1	27.2	−10.9	−12.8	−4.5	−17.3
D(t)-GB	−3.9	8.9	−1.8	3.2	−4.9	−1.7

[a] All values are in kcal/mol.

molecule with the other octahedral and tetrahedral rings surrounding the small cluster model. These interactions provide a significant contribution to the interaction energy of such adsorption systems, which is indicated by large differences in interaction energies between the large and small models. We conclude that for the calculation of the interaction energy of adsorption systems it is necessary to use a model of the mineral that is significantly larger than the target molecule and the calculations using small models provide only an approximate value of the interaction energy.

A comparison of interaction energies obtained from calculations using different LL methods reveals that the application of the HF/3-21G level of theory results in the larger value of the corrected interaction energy of calculated models of adsorption on the tetrahedral and octahedral surfaces (Table 7). This difference is larger for the adsorption on the tetrahedral surface (for example, 1 kcal/mol for the D(t)-GB model).

To gain more insight into the mechanism of the adsorption of GB and GD on the surface of dickite, we have investigated the results of the decomposition of the interaction energy using the scheme of Sokalski et al.[35] Table 8 presents these results for the inner part of the D(o)-GB and D(t)-GB adsorption models. The results in the case of adsorption on the octahedral surface follow chemical intuition. The most binding contribution to the interaction energy is composed of the electrostatic and delocalization counterparts. There is also a contribution that is not negligible and that originates from the correlation energy. This situation is typical for the formation of hydrogen bonds of any type.[45]

A much more interesting situation has been found for the adsorption on the tetrahedral surface. The results of energy decomposition analysis suggest that the total contribution to the interaction energy obtained at the SCF level is repulsive. This is in contrast to both the situation described above and the published data,[45] where the number of different hydrogen bonds was decomposed using the scheme of Morokuma and Kitaura.[46] However, all other components of the energy decomposition (related to the single hydrogen bond) are in the range of the published data[45] and the data described by us above (Table 8). Therefore, we concluded that for the adsorption of GB on the tetrahedral surface, in addition to the formation of six C−H···O hydrogen bonds, some quite strong electrostatic repulsions also exist between nonbonded atoms. An analysis of the geometrical parameters of the D(t)-GB complex suggests that the distance between the O1 atom and the two basal oxygen atoms of the tetrahedral side is less than 3 Å. We have also found that this type of contact does not exist for the adsorption of GB on the octahedral surface. Hence, we conclude that the source of the repulsive electrostatic interactions originates from

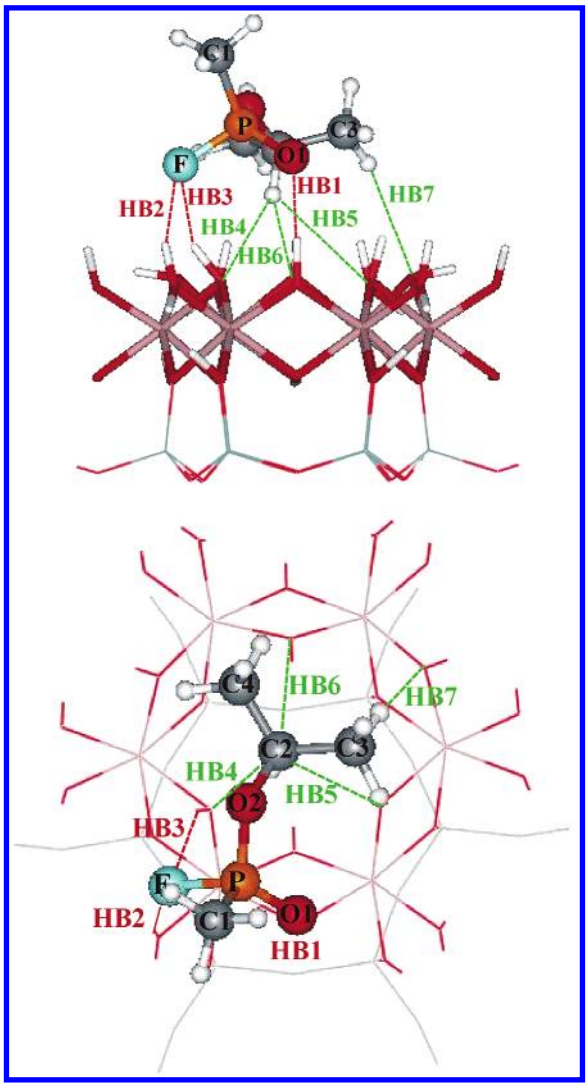

Figure 8. Dickite−sarin adsorbed system on the octahedral surface with a different optimized structure of the adsorbed molecule—D′(o)-GB. Two views of the cluster model in optimized geometry obtained using the ONIOM(B3LYP/6-31G(d,p):PM3) method.

the interactions of the O1 atom of GB with the two basal oxygen atoms of the tetrahedral surface of dickite.

3.3. Other Adsorption Complexes. One can see that the organic molecule can be located in several orientations on the dickite surface. The most electronegative F atom of GB and GD can also form hydrogen bonds with the octahedral surface. (The CH groups of the molecule play the main role in the formation of hydrogen bonds in the adsorption on the tetrahedral surface.) There are generally four main different initial orientations of sarin related to the active centers that could be involved in H bonds with the octahedral surface. The first one involves the orientation of the O1 atom toward the center of the octahedral ring. (This one has already been discussed.) Then both the O1 and fluorine atoms could be oriented toward the surface. Another configuration involves only the fluorine atom directed toward the center of the octahedral cavity. Finally, both the fluorine and the O2 atoms are oriented toward the surface.

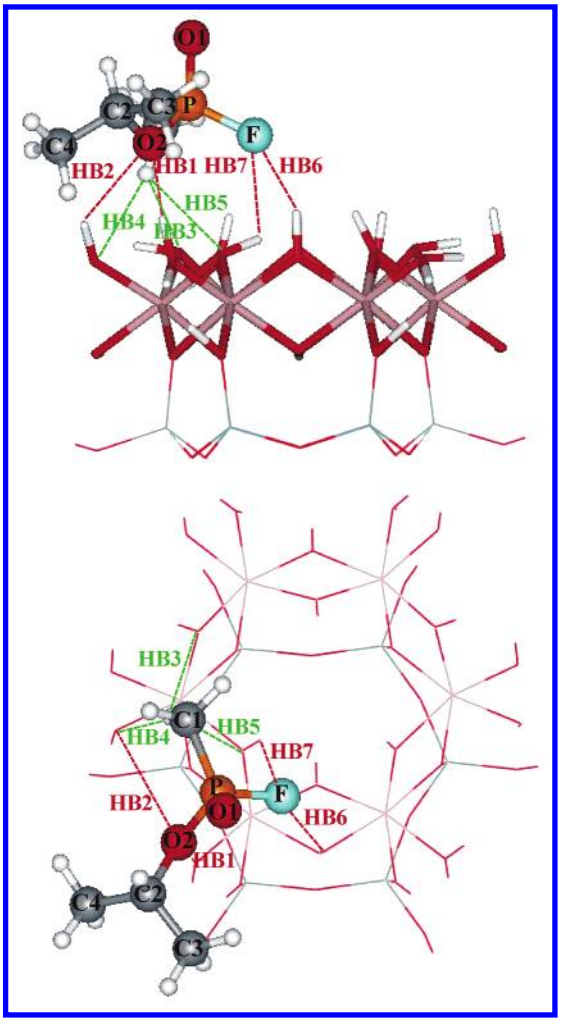

Figure 9. Dickite−sarin adsorbed system on the octahedral surface with a different optimized structure of the adsorbed molecule—D″(o)-GB. Two views of the cluster model in optimized geometry obtained using the ONIOM(B3LYP/6-31G(d,p):PM3) method.

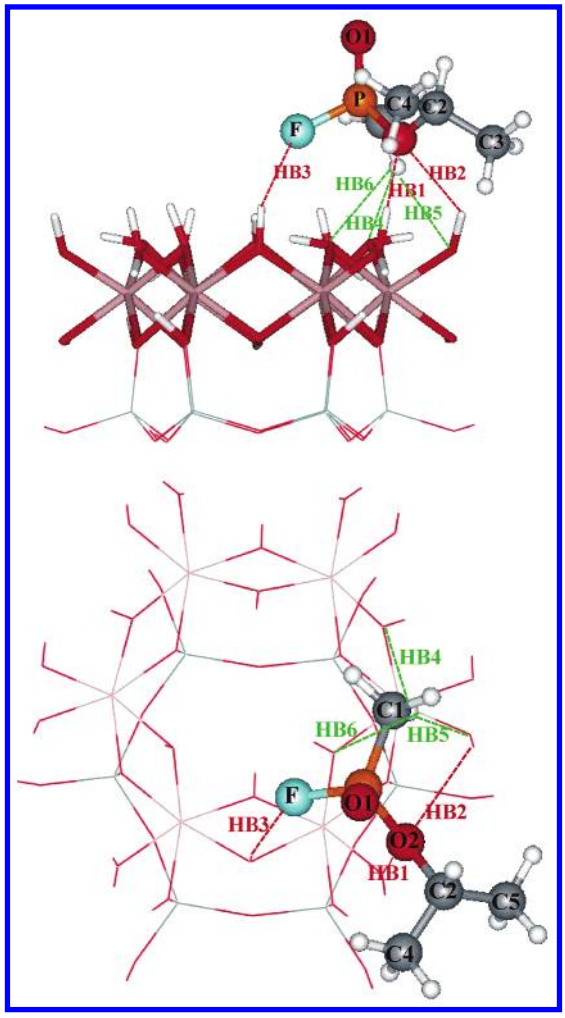

Figure 10. Dickite−sarin adsorbed system on the octahedral surface with a different optimized structure of the adsorbed molecule—D‴(o)-GB. Two views of the cluster model in optimized geometry obtained using the ONIOM(B3LYP/6-31G(d,p):PM3) method.

We have modeled all of these alternative orientations of sarin on the surface of dickite.

Let us discuss the structure of several other studied adsorption complexes with sarin on the octahedral surface. These structures of adsorbed GB are obtained using the ONIOM(B3LYP/6-31G(d,p):PM3) method and the D′(o)-GB, D″(o)-GB and D‴(o)-GB models with GB positioned above the center of the ring in such an initial orientation that (1) the fluorine and O1 atoms are directed toward the surface (D′(o)-GB), (2) the F atom is directed into the center of the octahedral cavity (D″(o)-GB), and (3) the O2 and fluorine atoms are oriented toward the surface (D‴(o)-GB model) (Figures 8−10). During optimization, sarin has moved from the central position above the cavity to the border of the ring because of the effort to form the maximum number of hydrogen bonds with surface hydroxyls. It is a structure that does not allow a large number of bonds to be created when sarin is in the middle position above the ring. One can see that the considered models differ in the characteristics of hydrogen bonds formed between the organic molecule and the mineral from the other models. In the D′(o)-GB model, the O1 atom (HB1) and in the D″(o)-GB model the O2 atom (HB1 and HB2) and fluorine (HB2 and HB3 in the D′(o)-GB model and HB6 and HB7 in the D″(o)-GB model) form H bonds with the surface hydroxyls of dickite. In the D‴-(o)-GB model, the O2 atom (HB1 and HB2) and the fluorine atom (HB3) create typical H bonds with the surface. In addition, the C−H groups of sarin form several H bonds with the oxygen atoms of the surface hydroxyls (HB4−HB7 in D′(o)-GB, HB3−HB5 in D″(o)-GB, and HB4−HB6 in D‴(o)-GB). The geometrical parameters and topological characteristics of these hydrogen bonds are presented in Table 9. The hydrogen bonds formed between the fluorine, O1, and O2 atoms and the surface hydroxyl groups are weaker (except HB1 in D″(o)-GB) in these new models than the hydrogen bonds formed with the O1 atom in the D(o)-GB system. It can be seen from the comparison of values of electron densities and the Laplacian of electron densities presented in Table 9. On average, the hydrogen bonds with fluorine are characterized by a value of ρ that is 2 times smaller than that for the hydrogen bonds with the O1 atom. Despite its electronegative character, the fluorine atom forms weaker H bonds with the surface in comparison with H bonds formed by the O1 atom. This can be caused by the large molecular volume of sarin, which does not allow the molecule to be oriented in such a way that H bonds with the fluorine atom will be more advantageous than H bonds with the P═O oxygen atom. The interaction energies predicted using the D′-(o)-GB and D″(o)-GB models are −10.7 and −10.6 kcal/mol, respectively, and that obtained using the D‴(o)-GB model is −11.1 kcal/mol. It is about 2 kcal/mol less than was found using the D(o)-GB model. This means that the interactions between

TABLE 9: Calculated ONIOM(B3LYP/6-31G(d,p):PM3) H···Y and X···Y[a] Distances, (Å) X−H···Y Angles (deg), and Electron Density Characteristics[b] ρ (au) and $\nabla^2\rho$ (au) of Hydrogen Bonds in the D-GB System[c]

	D′(o)-GB				D″(o)-GB			
	H···Y (X···Y)	X−H···Y	ρ	$\nabla^2\rho$	H···Y (X···Y)	X−H···Y	ρ	$\nabla^2\rho$
HB1	1.898 (2.867)	174.6	0.0270	0.0790	1.709 (2.701)	170.8	0.0414	0.1139
HB2	1.973 (2.924)	158.0	0.0185	0.0565	2.934 (3.728)	136.9	0.0038	0.0158
HB3	2.365 (3.125)	135.1	0.0094	0.0402	2.588 (3.336)	124.5	0.0083	0.0309
HB4	2.377 (3.413)	157.6	0.0123	0.0366	2.274 (3.340)	162.9	0.0169	0.0439
HB5	3.005 (3.762)	126.7	0.0034	0.0137	2.553 (3.226)	118.4	0.0092	0.0354
HB6	3.159 (3.618)	106.1	0.0046	0.0209	2.296 (3.154)	147.4	0.0092	0.0386
HB7	2.851 (3.876)	155.7	0.0049	0.0168	2.676 (2.862)	91.1	0.0100	0.0399
	D‴(o)-GB				D(o)-GB			
	H···Y (X···Y)	X−H···Y	ρ	$\nabla^2\rho$	H···Y (X···Y)	X−H···Y	ρ	$\nabla^2\rho$
HB1	1.694 (2.687)	171.8	0.0430	0.1182	2.061 (2.989)	161.1	0.0204	0.0652
HB2	2.881 (3.682)	137.6	0.0042	0.0173	2.106 (2.868)	134.7	0.0296	0.0887
HB3	2.218 (3.121)	155.3	0.0110	0.0420	2.154 (3.117)	174.7	0.0203	0.0592
HB4	2.570 (3.330)	125.4	0.00848	0.0315	2.609 (3.315)	121.3	0.0053	0.0208
HB5	2.310 (3.373)	162.1	0.0157	0.0409	2.329 (3.41)	167.7	0.0086	0.0239
HB6	2.515 (3.190)	118.5	0.0098	0.0375	2.686 (3.062)	99.5	0.0079	0.0296
HB7					2.751 (3.77)	154.5	0.0048	0.0191

[a] In parentheses. [b] Inner part, B3LYP/6-31G(d,p). [c] Octahedral side.

TABLE 10: Calculated ONIOM(B3LYP/6-31G(d,p):PM3) H···Y and X···Y[a] Distances (Å), X−H···Y Angles (deg), and Electron Density Characteristics[b] ρ (au) and $\nabla^2\rho$ (au) of Hydrogen Bonds in the D-GB System[c]

	D′(t)-GB				D(t)-GB			
	H···Y (X···Y)	X−H···Y	ρ	$\nabla^2\rho$	H···Y (X···Y)	X−H···Y	ρ	$\nabla^2\rho$
HB1	2.806 (3.870)	164.3	0.0047	0.0176	3.01 (3.794)	129.1	0.0033	0.0143
HB2	2.853 (3.712)	135.5	0.0045	0.0175	2.639 (3.706)	165.4	0.0075	0.0257
HB3	2.657 (3.675)	154.5	0.0067	0.0230	2.770 (3.588)	131.5	0.0069	0.0259
HB4	2.827 (3.663)	133.1	0.0049	0.0184	3.292 (3.975)	121.6	0.0033	0.0138
HB5					3.190 (3.915)	124.7	0.0036	0.0145
HB6					2.632 (3.967)	164.4	0.0083	0.0262
HB7								

[a] In parentheses. [b] Inner part, B3LYP/6-31G(d,p). [c] Tetrahedral side.

the O1 atom of GB and the surface hydroxyl groups are the most preferable in the stabilization of GB on the octahedral surface of dickite. This indicates that the O1 atom plays a crucial role in the stabilization of these molecules on the octahedral surface of dickite because such adsorption complexes are the most stable. Of course, to confirm this statement some calculations of the adsorption of GB and GD (in such an initial orientation that fluorine could be involved in H bonds) on the octahedral surface of dickite using a large cluster of the mineral should be performed.

In the case of the adsorption on the tetrahedral surface, the different local minima using the D′(t)-GB model were also found such that the R group of GB covers the ditrigonal cavity. (See Figure 11, which presents the optimized structure of GB obtained by using the D′(t)-GB model and the ONIOM(B3LYP/6-31G(d,p):PM3) method.) In this model, different numbers and strengths of hydrogen bonds were found (Table 10) compared to those of the D(t)-GB system. In the D′(t)-GB model, only four weak C−H···O hydrogen bonds are formed, which are on average characterized by smaller values of $\nabla^2\rho$ in comparison with those of the D(t)-GB model. According to these results and on the basis of the values of interaction energies obtained using these models, GB with the $-CH_3$ group directed into the center of the ditrigonal cavity is more stable. (The interaction energy obtained using the D′(t)-GB model is −1.9 kcal/mol.)

4. Conclusions

A study of the adsorption of sarin (GB) and soman (GD) on the octahedral and tetrahedral surfaces of dickite using the two-level ONIOM(B3LYP/6-31G(d,p):PM3) and ONIOM(B3LYP/6-31G(d,p):HF/3-21G) methods and the cluster model approximation has been performed.

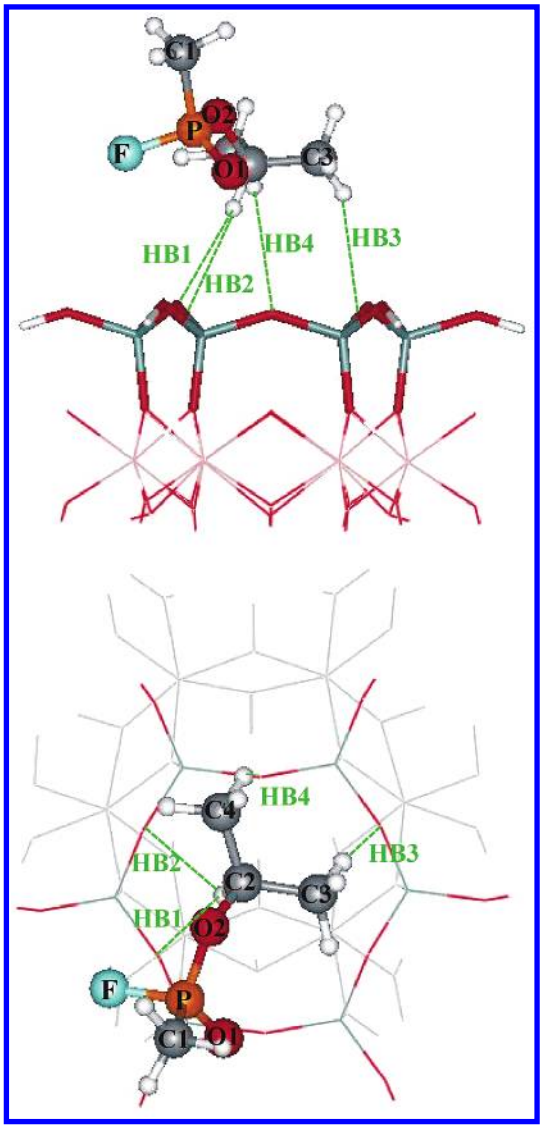

Figure 11. Dickite−sarin adsorbed system on the tetrahedral surface with a different optimized structure of the adsorbed molecule−D′(t)-GB. Two views of the cluster model in optimized geometry obtained using the ONIOM(B3LYP/6-31G(d,p):PM3) method.

The calculation using small and large models of the clay mineral results in similar positions and geometrical parameters of sarin and soman. Formally, GB and GD can be adsorbed on the octahedral and tetrahedral surfaces of dickite so that they cover the octahedral and ditrigonal cavities. An analysis of the topological characteristics of electron density distribution in the inner part of the D-GB and D-GD systems at the B3LYP/6-31G(d,p) level of theory reveals that the adsorption of sarin and soman on the surface of dickite occurs through the formation of multiple hydrogen bonds. These hydrogen bonds were found between the oxygen atom and the methyl groups of GB and GD and the hydroxyl groups (the adsorption on the octahedral surface) and between the methyl groups of GB and GD and the basal oxygen atoms (the adsorption on the tetrahedral surface).

The adsorption results in polarization and in changes in the geometric parameters of adsorbed molecules. This corresponds to the formation of attractive contacts between GB and GD and the surface of dickite. The polarization of the organic molecule is more significant in the case of adsorption on the octahedral side. The amount of electron density that is transferred from the mineral to sarin and soman is proportional to the binding strength.

Interaction energies of the adsorption system with the organic molecule on the octahedral surface are almost 2 times larger than the interaction energies of adsorption systems on the tetrahedral surface. Therefore, we conclude that sarin and soman will adsorb most preferably on the octahedral surface of dickite.

In the case of adsorption on the octahedral surface, an analysis of the interaction-energy components indicates the significant importance of electrostatic and delocalization binding contributions. In the case of adsorption on the tetrahedral surface, the contribution of the SCF term to the total interaction energy is repulsive. It originates from repulsive interactions between the P═O oxygen atom of sarin and the basal oxygen atoms of the tetrahedral surface of dickite. The stabilization of sarin and soman adsorbed on the tetrahedral surface is secured by the correlation forces.

The additional local minima of adsorbed sarin on the tetrahedral and octahedral surface of dickite were found. They are characterized by the different involvement of the fluorine atom in intermolecular interactions. H bonds are weaker in comparison with H bonds in which the P═O oxygen atom participates. These systems are less stable than already-discussed adsorption systems.

Acknowledgment. This work was facilitated by the support of the Office of Naval Research grant no. N00034-03-1-0116 and by the support of the Army High Performance Computing Research Center under the auspices of the Department of the Army grant no. DAAD19-01-2-0014 and the Army Research Laboratory Cooperative agreement no. DAAH04-95-2-0003/ contract number DAAH04-95-C-0008, the content of which does not necessarily reflect the position or the policy of the government and no official endorsement should be inferred.

References and Notes

(1) *The Chemistry of Clays and Clay Minerals*; Newman, A. C. D., Ed.; Mineralogical Society Monograph No. 6; Longman Scientific & Technical: London, 1987.

(2) Bailey, S. W. *Structures of Layered Silicates*; In Crystal Structures of Clay Minerals and their X-ray Identification; Brindley, G. W., Brown, G., Eds.; Mineralogical Society: London, 1980; pp 6−28.

(3) Bates, R. L. *Stone, Clay, Glasses: How Building Materials are Found and Used*; Erslow: New York, 1987.

(4) Grim, R. E. *Clay Mineralogy*, McGraw-Hill: New York, 1953.

(5) http://www.n-b-c-warfare.com/chemical/lewisite.htm − Nuclear Chemical Biological Warfare.

(6) Benco, L.; Tunega, D.; Hafner, J.; Lischka, H. *Am. Miner.* **2001**, *86*, 1057.

(7) Bryant, P. J. R.; Ford-Moore, A. H.; Perry, B. J.; Wardrop, A. W. H.; Walkins, T. F. *J. Chem. Soc.* **1960**, 1553.

(8) Walker, A. R. H.; Suenram, R. D.; Samuels, A.; Jensen, J.; Ellzy, M. W.; Lonchner, J. M.; Zeroka, D. *J. Mol. Spectrosc.* **2001**, *297*, 77.

(9) Kaczmarek, A.; Gorb, L.; Sadlej, A. J.; Leszczynski, J. *Struct. Chem.* 2003, submitted for publication.

(10) Takimoto, K.; Ito, K.; Mukai, T.; Okada, M. *Environ. Sci. Technol.* **1998**, *32*, 3907.

(11) Bowen, J. M.; Powers, C. R.; Ratcliffe, A. E.; Rockley, M. G.; Hounslow, A. W. *Environ. Sci. Technol.* **1988**, *22*, 1178.

(12) Bowen, J. M.; Compton, S. V.; Blanche, M. S. *Anal. Chem.* **1989**, *61*, 2047.

(13) Levesque, M.; Schnitzer, M. *Soil Sci.* **1967**, *103*, 183.

(14) Hance, R. J. *Pest. Sci.* **1976**, *23*, 363.

(15) Shoval, S.; Yariv, S. *Clays Clay Miner.* **1979**, *27*, 19.

(16) Sprankle, P.; Meggitt, W. F.; Penner, D. *Weed Sci.* **1975**, *23*, 229.

(17) Morillo, E.; Undabeytia, T.; Maqueda, C. *Environ. Sci. Technol.* **1997**, *31*, 3588.

(18) McConnell, J. S.; Hossner, L. R. *J. Agric. Food Chem.* **1985**, *33*, 1075.

(19) Glass, R. L. *J. Agric. Food Chem.* **1987**, *35*, 497.

(20) Michalkova, A.; Gorb, L.; Ilchenko, M.; Leszczynski, J. To be submitted for publication.

(21) Kataoka, M.; Tsunoda, N.; Ohta, H.; Tsuge, K.; Takesako, H.; Seto, Y. *J. Chromatogr., A* **1998**, *824*, 211.

(22) Vermilion, W. D.; Crenshaw, M. D. *J. Chromatogr., A* **1997**, *770*, 253.
(23) Kataoka, M.; Tsuge, K.; Takesako, H.; Hamazaki, T.; Seto, Y. *Environ. Sci. Technol.* **2001**, *35*, 1823.
(24) D'Agostino, P.; Hancock, J. R.; Provost, L. R. *J. Chromatogr., A* **2001**, *912*, 291.
(25) Murashov, V. V.; Leszczynski, J. *J. Phys. Chem. A* **1999**, *103*, 1228.
(26) Hartzell, C. J.; Cygan, R. T.; Nagy, K. L. *J. Phys. Chem. A* **1998**, *102*, 6722.
(27) Svensson, M.; Humbel, S.; Froese, R. D. J.; Matsubara, T.; Sieber, S.; Morokuma, K. *J. Phys. Chem.* **1996**, *100*, 19357.
(28) Frisch, M. J.; Trucks, G. W.; Schlegel, H. B.; Scuseria, G. E.; Robb, M. A.; Cheeseman, J. R.; Zakrzewski, V. G.; Montgomery, J. A., Jr.; Stratmann, R. E.; Burant, J. C.; Dapprich, S.; Millam, J. M.; Daniels, A. D.; Kudin, K. N.; Strain, M. C.; Farkas, O.; Tomasi, J.; Barone, V.; Cossi, M.; Cammi, R.; Mennucci, B.; Pomelli, C.; Adamo, C.; Clifford, S.; Ochterski, J.; Petersson, G. A.; Ayala, P. Y.; Cui, Q.; Morokuma, K.; Malick, D. K.; Rabuck, A. D.; Raghavachari, K.; Foresman, J. B.; Cioslowski, J.; Ortiz, J. V.; Stefanov, B. B.; Liu, G.; Liashenko, A.; Piskorz, P.; Komaromi, I.; Gomperts, R.; Martin, R. L.; Fox, D. J.; Keith, T.; Al-Laham, M. A.; Peng, C. Y.; Nanayakkara, A.; Gonzalez, C.; Challacombe, M.; Gill, P. M. W.; Johnson, B. G.; Chen, W.; Wong, M. W.; Andres, J. L.; Head-Gordon, M.; Replogle, E. S.; Pople, J. A. *Gaussian 98*, revision A.7; Gaussian, Inc.: Pittsburgh, PA, 1998.
(29) Becke, D. *J. Chem. Phys.* **1993**, *98*, 5648.
(30) Yang, L. W.; Parr, R. G. *Phys. Rev. B* **1998**, *37*, 785.
(31) Stewart, J. P. *J. Comput. Chem.* **1989**, *10*, 209.
(32) Stewart, J. P. *J. Comput. Chem.* **1989**, *10*, 221.
(33) Joswig, W.; Drits, V. A. *N. Jb. Miner. Mh.* **1986**, 19.
(34) Boys, S. F.; Bernardi, F. *Mol. Phys.* **1970**, *19*, 553.
(35) Sokalski, W. A.; Roszak, S.; Pecul, K. *Chem. Phys. Lett.* **1988**, 153.
(36) Jeziorski, B.; van Hemert, M. C. *Mol. Phys.* **1976**, *31*, 713.
(37) Chalasinski, G.; Szczesniak, M. M. *Mol. Phys.* **1988**, *63*, 205.
(38) Bader, R. W. F. *Atoms in Molecules: A Quantum Theory;* Oxford University Press: Oxford, England, 1990.
(39) Michalkova, A.; Tunega, D.; Turi Nagy, L. *J. Mol. Structure: THEOCHEM* **2002**, *581*, 37.
(40) Tunega, D.; Haberhauer, G.; Gerzabek, M. H.; Lischka, H. *Langmuir* **2002**, *18*, 139.
(41) Tunega, D.; Benco, L.; Haberhauer, G.; Gerzabek, M. H.; Lishka, H. *J. Phys. Chem. B* **2002**, *106*, 11515.
(42) Koch, U.; Popelier, P. L. A. *J. Phys. Chem.* **1995**, *99*, 9747.
(43) Popelier, P. A. L. *J. Phys. Chem. A* **1998**, *102*, 1873.
(44) Desiraju, G. R. *Acc. Chem. Res.* **1991**, *24*, 290.
(45) Gu, Y.; Kar, T.; Scheiner, S. *J. Am. Chem. Soc.* **1999**, *121*, 9411.
(46) Morokuma, K.; Kitaura, K. In *Molecular Interactions*; Ratajczak, H., Orville-Thomas, W. J., Eds.; Wiley: New York, 1980; Vol. 1, p 21.